

Modelling of a Heat Conduction Calorimeter Used in Cement Plant Automation

Hassan Alzeidi



LUND
UNIVERSITY

Department of Automatic Control

MSc Thesis
TFRT-6186
ISSN 0280-5316

Department of Automatic Control
Lund University
Box 118
SE-221 00 LUND
Sweden

© 2022 by Hassan Alzeidi. All rights reserved.
Printed in Sweden by Tryckeriet i E-huset
Lund 2022

Abstract

A model is used to describe a system physically or mathematically and to give information about changes in the system variables. Physical knowledge about the system and its quantities can be useful to build a physical model obeying the laws of nature. However, if the system is to be regarded as a black box with only input and output signals, system identification can be used to fit a mathematical model to describe the relation between the signals. The signals are usually physical quantities but the estimated model parameters do not necessarily reflect physical aspects of the system. The goal of estimating a model is either to calculate the effect given the cause, such models are called forward or direct models, or to calculate the cause given the effect, which is the objective of this thesis. These models are called inverse models and are widely used in heat conduction problems, e.g., estimating the heat flow rate at the source given measured temperature at a point. In this thesis the goal is to estimate the true heat flow rate from the hydration reaction in a cement sample when mixed with water from heat rate measurements in the isothermal calorimeter I-Cal Flex. The problem with such measurement is that it starts only after about 20-30 seconds, which is the time it takes for mixing the water and cement in an ampoule and charging it in the calorimeter. Under that time the cement sample temperature rises due to heat produced from the chemical reaction. The measurement process is automated in a robot called PolabCal and the measurement signal could possibly be used to control cement plants. The problem is that the measurement both includes the heat rate from the over-temperature that sample gained prior charging in the calorimeter and information about the dynamics of the instrument. There is therefore an interest in the pure heat rate from the cement hydration reaction as it is believed to be more informative than the measurement signal. Estimating the inverse model in this thesis was made by evaluating three methods; to estimate a forward model then to invert it, to estimate an inverse model directly from inputs and output measurements, and lastly to build a physical forward model and then use it to calculate the input.

Acknowledgements

My deepest gratitude to my supervisor at the Division of Building Materials, professor Lars Wadsö for seeing potential in me to carry out this thesis project. Thank you for the plenty of time, patience and constant support you gave me. It was very inspirational observing your work ethic and passion towards what you do and it was a pleasure doing this project under your guidance.

All the appreciation to my supervisor professor Anders Rantzer at the Department of Automatic Control. The regular meetings at your office were always helpful and informative. Your new ideas and guidance always carried this project forward.

I also want to thank my industrial supervisor Dr. Michael Enders at Thyssenkrupp Industrial Solutions for taking care of us under the trip and teaching me about the cement industry. It was always fascinating listening to you and how much deep knowledge you have in many different fields. Thank you to the laboratory team at Dyckerhoff in Lengerich for letting us work with their PolabCal and showing us around at the plant.

I want to thank my parents for supporting me not only through this project but through my whole life. I love you, and I appreciate you.

Last but not least, I want to thank my dear wife for taking care of me and supporting me through these 5 months. I love you and I appreciate you.

Nomenclature

Symbols

S_F	Estimated forward model
S_F^{-1}	Inverse of the forward model
S_I	Estimated inverse model
S_{FI}	Estimated inverse model from input data and simulated output from the forward model
P_{in}	Electric power input
U	Applied voltage
y_1, u_1	These appear in plots and refer to the input and output signals of the system, the subscripts indicate that it is a SISO system
q	Forward shift operator
Q	Heat rate
c	Specific heat capacity
m	Mass
T_s	Sample period
R	Resistance
$G(q)$	Input/output model
$H(q)$	Noise model
\hat{y}	Predicted output
θ	Model parameters
φ	Regressor vector
Bi	Biot number
k	Thermal conductivity
h	Heat transfer coefficient
L	Characteristic length

Abbreviations

SITB	System Identification Toolbox
FEM	Finite Element Modelling
LHCM	Lumped Heat Capacity Modelling
LTI	Linear time-invariant
RSS	The residuals of the squared sum
SNR	Signal to Noise Ratio
RMS	Root Mean Squared Error
SISO	Single Input Single Output

Contents

1. Introduction	11
2. Background	13
2.1 Portland cement	13
2.2 Carbon Dioxide Emission	13
2.3 Hydration of Cement	14
2.4 Cement Plant Control	14
2.5 The Calorimetric Measurement	16
2.6 Isothermal Calorimetry	17
3. System Identification and Modelling	19
3.1 System Identification	20
3.2 The cycle of identification	20
3.3 Models	21
3.3.1 Linear models	22
3.4 Data Collection	23
3.4.1 Identifiability	23
3.4.2 Signal to Noise Ratio (<i>SNR</i>)	24
3.5 Model Calculation	24
3.6 Model Validation	24
3.7 Physical Modelling	24
3.7.1 Lumped capacity systems	25
3.8 The Inverse	27
3.8.1 Difficulties with the inverse	27
4. Implementation of the Forward Inverse Model and the Estimated Inverse Model	28
4.1 Collecting data	28
4.1.1 Design limitations	28
4.1.2 Designing the experiment	29
4.1.3 Selecting first model structure	30
4.1.4 Developing the Model	32
4.1.5 Inverting the Forward Models	35

4.1.6	Direct estimation of the Inverse Model	37
5.	Physical Modelling Implementation	40
5.1	Nodal Models	40
5.2	4-nodes Model	41
5.2.1	Sensitivity Analysis	42
5.3	5-nodes Model	44
5.4	3-nodes Model	45
5.5	Comparison	46
5.6	Calculating the Inverse	46
6.	Discussion	49
	Bibliography	51

1

Introduction

Cement plants make use of isothermal calorimetry to control the production quality. An isothermal calorimeter can measure the heat rate in a cement sample when it is mixed with water. The chemical reaction between the water and cement by which heat is produced is called the hydration reaction and is characterized by its pattern of heat release, which starts when the cement comes in contact with water. Cement plant laboratories do have calorimeters, but they are mainly used in product development and trouble-shooting, not for control of the daily operation. However, ThyssenKrupp Industrial Solutions have developed an automated I-Cal Ultra calorimeter that should give results within 20 min of measurements, with the aim of extracting parameters from these measurements that should be useful to control the cement manufacturing process. Charging cement samples in the calorimeter is done in a chamber with a regulated temperature. It is important that the cement sample, after it is mixed with water is inserted in the instrument as soon as possible to capture most of the heat rate. This measured signal from the calorimeter could be used in process control, but it is a signal that contains information on both the cement hydration and the thermal inertia of the calorimeter. If it is possible to remove the calorimeter information, to have only the cement hydration result, this would improve the usefulness of the data.

The goal of this thesis is to try to reconstruct the original heat rate by means of using inverse modelling. While there is lots of literature and advancement in forward modelling which is estimating a model that explains the relation from the input to the output, inverse modelling is still a field that expands.

This thesis starts with a chapter on cement production, cement compounds, the hydration reaction, PolabCal and isothermal calorimetry. In chapter 3, some methodology on physical modelling and system identification will be introduced. This chapter explains popular linear models used and discusses considerations around building a linear model. Lumped heat capacity modelling is also explained. Chapter 4 discusses the mathematical implementation of the forward model and its mathematical inverse model using system identification. In the same chapter the inverse model is directly estimated from data using two methods; classical linear models and IARX. In chapter 5, the physical model is implemented using LHCM, the inverse is calcu-

Chapter 1. Introduction

lated and the results are presented. The last chapter is a general discussion of the results.

2

Background

2.1 Portland cement

Cement is an essential compound to bond sand, stone and building blocks in building and civil engineering. The cement of interest in construction and making of concrete is known as Portland cement and is made from limestone and clay that are ground and mixed in certain proportions and then burned in rotating kilns at temperatures around 1450 °C. At this temperature, clinker in the form of pebbles is produced and it contains the four main compounds listed in table 2.1. However, the clinker has to be rapidly cooled down to conserve the reactive compounds. Portland cement is then made by grinding the clinker together with 2-3 % gypsum to regulate the setting time and control the reaction of C₃A [9]. The final product is a fine powder with a particle size of about 10 μm that can be mixed with water to form a cement paste that within few hours starts to react to form a harden cement paste that is the binder that holds together the sand and rocks in concrete.

Compound	Oxide composition	Abbreviation
Tricalcium silicate	3CaO·SiO ₂	C ₃ S
Dicalcium silicate	2CaO·SiO ₂	C ₂ S
Tricalcium aluminate	3CaO·Al ₂ O ₃	C ₃ A
Tetracalcium aluminoferrite	4CaO·Al ₂ O ₃ ·Fe ₂ O ₃	C ₄ AF

Table 2.1 Main compounds of Portland Cement [3] .

2.2 Carbon Dioxide Emission

Cement production is a large contributor to climate change as a result of being the most produced building material world wide. The production process involves high emissions of carbon dioxide, 40% from the chemical calcination of limestone and 50% from burning fossil fuel to heat the kilns. For every kg of Portland cement produced about 0.9 kg of carbon dioxide is emitted. With more than 4 billion tonnes

of cement produced every year cement production accounts for above 8% of global carbon dioxide emission and it is predicted to increase to 5 billion tonnes over the next 30 years. Therefore, for cement plants to be in line with the *Paris Agreement* on climate change, the annual carbon dioxide emission must be reduced by 16% by the year 2030 while the production increases. To reach this goal optimizing cement production plays a key role and is demonstrated today in changing the fuels and in using alternative materials to blend with the clinker such as fly ash and blast furnace slag that also react as they are activated by the Portland cement [6]. Optimizing the design of concrete structures to use a minimal amount of cement is also another method. In the future carbon capture and storage techniques might also be used at cement plants.

2.3 Hydration of Cement

The reaction of cement with water in which the hard mass of cement paste is formed is called hydration. As all hydration reactions produce heat, measurement of heat rate from the hydration reaction has been a popular method to visualize and analyse cement reactions. The most common instrument for heat rate measurements in cement industry and cement research is isothermal calorimetry, see fig. 2.4. Hydration is a multi-step process described schematically in fig. 2.2. It starts with the initial reactions (I) of very high heat rate which then is followed by the induction period (II) during which the concrete can be transported and cast at the construction site.

The main strength forming reaction (III) starts typically after 2 h. It accelerates, peaks and then decays (IV). The hydration reactions continue as long as there are unhydrated cement and water although at a slower and lower rate. The most reactive clinker compound is C_3A . It hydrates early — during phase (I) — together with the sulfate to form the compound ettringite, which does not lead to the hardening of cement. The hard product of hydration called C-S-H is mainly produced by the reaction of the main compound, C_3S in phase (III and IV). In the long term C-S-H is also produced at a much slower rate from the reaction of C_2S during phase (IV). C_4AF hydrates slowly and does not contribute much to the strength properties.[3]

2.4 Cement Plant Control

There are different measured parameters used to control a cement plant production: measuring the amount of certain compounds and elements and the particle size distribution. These parameters are typically measured every hour in central automated laboratories on production samples. None of the above metrics concerns the use of cement, i.e., its hydration properties, which are tested by measuring the strength of a standard mortar sample after 24 h of hydration.

In need of a faster way of assessing the reactivity of cement in real-time, the exothermic heat rate of hydration is analysed in isothermal calorimeters. The

strength develops in the second peak (II) that starts after several hours from the moment sand and water is mixed which is still a slow process that is difficult to utilise to control the plant. However, it is believed that the first peak carries information about the second peak. This is why ThyssenKrupp Industrial Solutions and Calmetrix have developed an automated isothermal calorimeter, PolabCal, that can be used in a cement plant laboratory to produce data on the reaction between cement and water quickly enough to be used for process control. In the PolabCal, a robot quickly mixes cement and water in a plastic vial and places the vial in an isothermal calorimeter that measures the heat flow from the sample in the vial. The robot operates inside a chamber with a regulated temperature equal to that of the calorimeter, see fig. 2.1. The PolabCal uses all 8 channels in the calorimeter and it takes measurements hourly all year long.

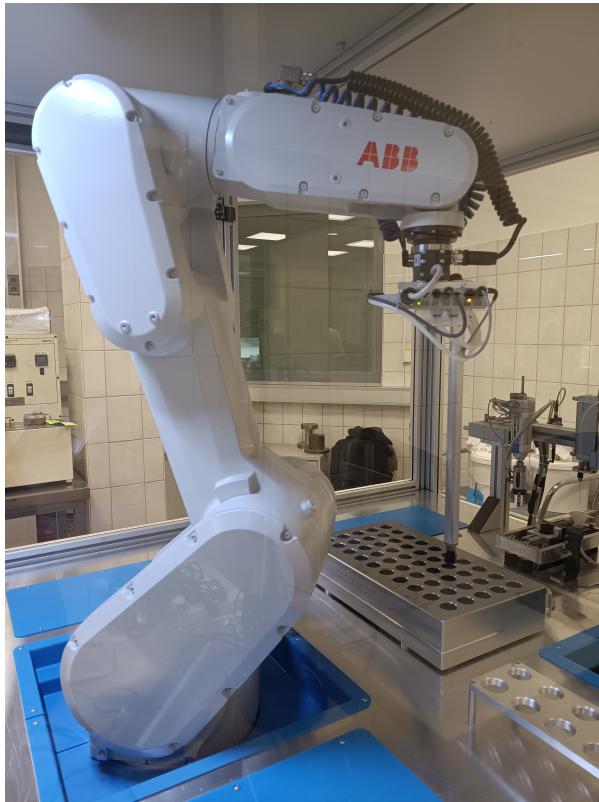


Figure 2.1 PolabCal robot arm inside the chamber.

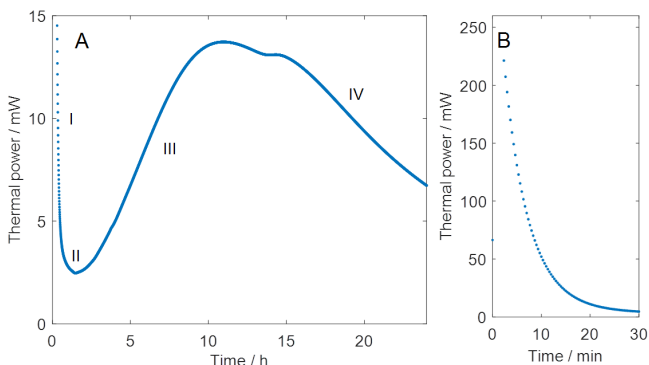


Figure 2.2 Thermal power of hydration per sample (5.5g cement and 2.75 water).

2.5 The Calorimetric Measurement

The cement measurement is typically not more than 20 min long see fig. 2.2 (B). A problem with this approach is that the calorimeter has a thermal inertia, so the signal from the calorimeter (the heat flow) does not represent the true heat production rate (thermal power) of the sample, but rather a sum of the true heat production from the time the vial was charged in the calorimeter and heat rate due to the initial temperature difference between the sample and calorimeter. The temperature difference is caused by the heat production of the hydration reaction prior charging into the instrument. One can also measure solely the the heat rate due to temperature difference between the calorimeter and a sample by using a sand and water sample. If such sample is kept at a temperature higher than the calorimeter for a while and than charged in the calorimeter one will observe a heat rate signal, see fig.2.3

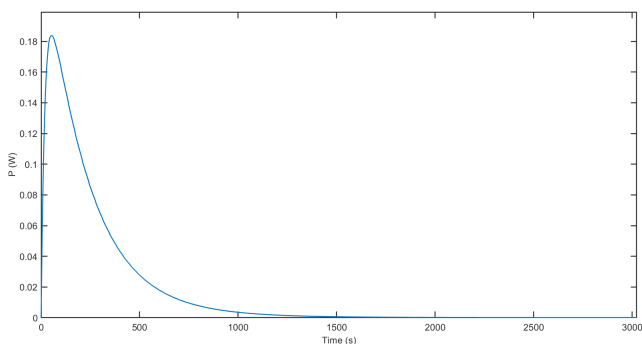


Figure 2.3 Measurement from sand and water sample with an initial temperature higher than the calorimeter).

The aim of this project is therefore to develop a thermal model of the calorimeter so that the measured heat flow can be recalculated to thermal power in the sample, i.e., to remove the influence of the instrument from the result, so that the result only includes information about the cement hydration process. Because of the initial over-temperature the cement sample gains from the heat production, the temperature of the sample, from the time of charging into the instrument, is also

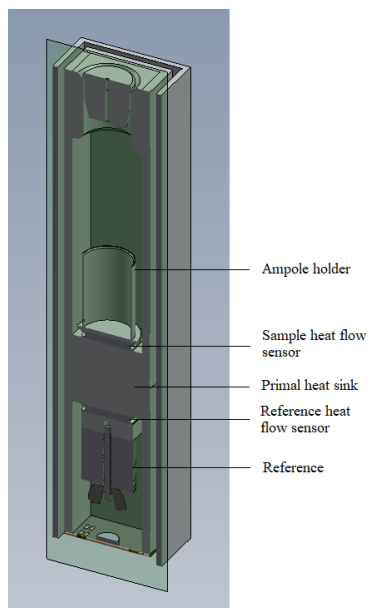
2.6 Isothermal Calorimetry

As mentioned above, one means of monitoring cement hydration is measuring the heat flow of the reaction using isothermal calorimetry. An isothermal calorimeter is a tool which measures rate of the heat flow produced in a sample at constant temperature, thus the term isothermal. The sample is charged into an ampoule that in turn is inserted in an ampoule holder which is in contact with a heat sink at a regulated temperature. Between the heat sink and the ampoule holder is a heat flow sensor that measures heat flow according to the Seebeck principle. However, using only this structure makes the system susceptible to noise, therefore all isothermal calorimeters use the twin principle, i.e. they all use a reference sample of similar thermal properties as the sample, especially heat capacity, except it does not produce heat.

The heat flow from the reference is subtracted from the heat flow from the sample and noise is thereby canceled. The calorimetric instrument used in the Polab Cal is called I-Cal Ultra and has 8 channels, see fig. 2.4.



(a) I-Cal Ultra calorimeter by Calmetrix.



(b) A single channel of I-Cal Ultra (28.3 × 6.35 cm)

Figure 2.4 I-Cal Ultra

3

System Identification and Modelling

A system is generally speaking an object whose properties is a subject of study. This broad definition could then be applied to all reality around us, the solar system, an airplane, a vehicle, food chain systems etc. For a food chain system in nature an interesting question could be: how long would a certain herbivore species last if the carnivore species number rises. Such a question could be answered experimentally, through disturbing the system and observing it. In fact, experimentation has been the main method of natural science to seek answers about system properties but it has its limitations:

- It is expensive: e.g. changing one part of a production machine multiple times leads to unusable products.
- It is dangerous: e.g. testing a vehicle brake system.
- The system does not exist yet: e.g. when designing an airplane one wants to test the effects of different shapes on the aerodynamics.

Especially for the last point, models of a system are crucial to study the properties of the system. A model of a system is thus a limited representation of a system that helps study the system without carrying out experimentation. It is limited because it does not give information about the whole system, but rather only a part of it which is the subject of interest. For example, an aerodynamic model of an airplane might not provide information about the aircraft fuel consumption. There are different types of models; physical models and mathematical models, both of which will be used for the calorimeter of study. With a physical model some physical properties of the system are known and used as subsystems that follow the laws of nature; e.g. when a resistor is connected to a voltage source, Ohm's law is observed and that gives information about the current. Mathematical models describe the system through mathematical equations between quantities like temperature and heat flow.

3.1 System Identification

System identification uses observation of the system in order to fit the model's properties to those of the system. This method of modeling often complements the physical model. As mentioned above, physical models are based on laws of nature which are mathematical models which once were observed. In order to introduce system identification more distinctly as a method of model design one should view a system as an object in which variables interact and produce a signal of interest called the output. The system itself can be disturbed by the user through inputs to produce a desirable output but also by undesirable signals that are called disturbances, that are either directly measurable or observed through the output. An example of a system viewed as interacting variables is a drone. Applying a varied current (input) to the motors of the drone causes a varied altitude (output) which is also affected by disturbances from the wind. To identify a model of a system it is assumed that the relationship between the signals of the system has a mathematical structure. The degree of complexity of the mathematical model depends on the system and the intended use of the system. The mathematical representation could be a system of differential or difference equations that could be characterized as being linear/non-linear, time continuous/time discrete and stochastic/deterministic etc. The first method adopted to build a model is to break up the system into several physical subsystems whose properties are understood from previous experimentation and empirical work. The subsystems are then joined together to form the whole system either through a system of differential equations or through element blocks according to a software. The other method is experimental and therefore also data dependent. The input and output data are then used to fit the pre-determined mathematical model through data analysis software.

3.2 The cycle of identification

The identification process is a repeated procedure in which a model structure is selected, the best model is estimated and finally validated. The common steps in such procedure can be summarized as follows (see fig. 3.1):

- Experiment design to collect input/output data.
- Analyzing the data. Usually the data is firstly detrended and means are removed. Sometimes even pre-filtering is applied to enhance certain frequencies. Resampling the data can also be useful.
- Selecting the model structure of which the parameters are estimated.
- According to a given criteria compute the best model in the set of models.
- Examining the model by analysing its model fit and correlation functions.

- If the model meets the criteria stop, otherwise test a different model structure, a different estimation method or even work with different design experiments.

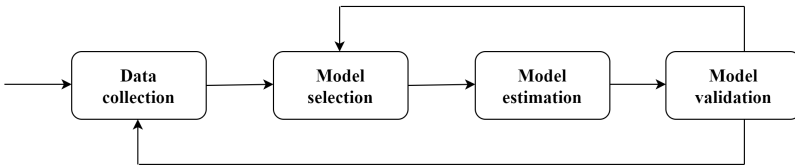


Figure 3.1 System Identification cycle.

3.3 Models

As mentioned, models are used to give information about the relationship between the system's observed variables. They are not meant to simulate the true system perfectly but rather give a decent description of certain aspects of interest. The data recorded from system operation as input and outputs are key for the modeling procedure. However choosing a model structure that relates the input and output and can be challenging. Prior physical and mathematical knowledge of the system is essential to give an intuitive idea about the structure and can be usefully utilized at this stage. Perhaps the most general model structure is the difference equation:

$$\begin{aligned} y(t) + a_1y(t-1) + \dots + a_{n_a}y(t-n_a) \\ = b_1u(t-1) + \dots + b_{n_b}u(t-n_b) + e(t) \end{aligned} \quad (3.1)$$

This expression can be interpreted as that the output depends on previous output and input observations. How many past observations that are used determines the degree of the difference equation and it is presented discretely as most data is collected by sampling. Equation 3.1 can take the matrix form:

$$A(q)y(t) = B(q)u(t) + e(t) \quad (3.2)$$

G and H being:

$$G(q, \theta) = \frac{B(q)}{A(q)}, \quad H(q, \theta) = \frac{1}{A(q)} \quad (3.3)$$

The model structure represented by equation 3.1 is called an ARX-model (auto regression with exogenous/extra inputs) as the model output depends on past output and input values.

3.3.1 Linear models

If a system is believed to be linear and time-invariant there is a set of linear model structures in which the search for a suitable model can start. A linear time-invariant model is characterized by its impulse response and the spectrum of its disturbance and stochastically maybe even the probability density function (PDF) of the disturbance. A model of such takes the form:

$$y(t) = G(q)u(t) + H(q)e(t) \quad (3.4)$$

with

$$G(q) = \sum_{k=1}^{\infty} g(k)q^{-k}, \quad H(q) = \sum_{k=1}^{\infty} h(k)q^{-k} \quad (3.5)$$

Thus, a linear model is specified by the functions G and H (e is assumed to be Gaussian). Each unique model from the set of models is characterized by the coefficients that enter the function which are determined by the identification procedure. As before these coefficients are denoted by θ and can be seen in the model predictor form:

$$\hat{y}(t|\theta) = H^{-1}(q, \theta)G(q, \theta)u(t) + [1 - H^{-1}(q, \theta)]y(t) \quad (3.6)$$

As the predicted data is essentially calculated, one denotes the model output instead with \hat{y} . From the basic model structure one notices two key vectors, the parameter vector and the data vector $\varphi(x)$ which is called the *regression* vector as the model regresses to past signal values. Of course, the regressors can also take a non-linear form, include disturbance vectors and can be extended to multiple inputs and outputs depending on the application. A common way of parametrizing G and H is to represent them as rational functions and there is a family of such transfer functions that are used in the field. Different transfer functions or structure setups emphasize different characteristics of the system to be caught. If the error term is to be considered insignificant the predictor term could thus be written as:

$$\hat{y}(t|\theta) = \theta^T \varphi(t) = \varphi^T(t) \theta \quad (3.7)$$

ARMAX. One of the disadvantages of the ARX model is the inflexibility in describing the disturbance term e , i.e., the Gaussian noise enters the dynamics of the systems only through the denominator. If instead the white noise is expressed as a moving average (MA) the model becomes thus:

$$A(q)y(t) = B(q)u(t) + C(q)e(t) \quad (3.8)$$

As in the previous model structures discussed above, the polynomial A is a common factor between the input and disturbance. To add more freedom to the model both G and H could be parameterized independently.

Box-Jenkins Model (BJ). A Box-Jenkins model structure takes the form:

$$y(t) = \frac{B(q)}{F(q)}u(t) + \frac{C(q)}{D(q)}e(t) \quad (3.9)$$

General Model. A model structure that could generally describe all the previous structures is:

$$A(q)y(t) = \frac{B(q)}{F(q)}u(t) + \frac{C(q)}{D(q)}e(t) \quad (3.10)$$

Depending on which of the five polynomials that are used, one can construct 32 different model sets from equation (12). The output could also be delayed by several samples when input is applied. Accounting for delay, equation 3.10 becomes:

$$A(q)y(t) = q^{-n} \frac{B(q)}{F(q)}u(t) + \frac{C(q)}{D(q)}e(t) \quad (3.11)$$

IARX. Especially for inverse modelling IARX is a novel method [4] that uses both past and future exogenous inputs to directly estimate the inverse model according to:

$$u[k] = - \sum_{i=1}^{n_a} a_i u[k-1] + \sum_{i=0}^{n_b-1} b_i y[k-1] + \sum_{i=1}^{n_c} c_i u[k+1] \quad (3.12)$$

3.4 Data Collection

Data acquisition for system excitation is the first step and the most important step in system identification. It is the quantity and quality of the data that decides how much of the the dynamics is captured and in discrete time systems it is dependent on three key factors: the type of the input, the type of the hold device, and the sampling rate. Good input data is tied with the notion of identifiability and informative data.

3.4.1 Identifiability

The ability to identify a model precisely and uniquely is essentially dependent upon:

- The model: existence of a unique one-to-one mapping between the model and parameters.
- The estimation method: the ability to estimate the "true" model if infinite samples are available.
- The input experiment: if the input contains sufficient information to distinguish between two candidate models and if the SNR is high enough.

Luckily, for linear time-invariant systems, identifiability is guaranteed if the input is persistently exciting[7]. This means that the input should contain almost all frequencies but since that is not realizable, one seeks to cover as many frequencies as possible at the region of operation. Such input is satisfied if it is quasi stationary and if [1]:

$$\gamma_{uu}(\omega) > 0, \text{ for almost all } \omega \quad (3.13)$$

3.4.2 Signal to Noise Ratio (SNR)

SNR measures the relative contribution of deterministic and stochastic effects of a signal, and it is explained mathematically in equation 3.14:

$$SNR = \frac{\sigma_{Signal}}{\sigma_{Noise}} \quad (3.14)$$

Intuitively, a model should explain variations in the signal (true response). If noise is heavily embedded in the signal it thereby contributes to the variations of the output and as a result effects of the input is weakened. Therefore to estimate the parameters of a model precisely the strength of the signal should be significant relative to the noise.

3.5 Model Calculation

The model parameter can be calculated by different methods the most common of which is the least squares method. The least squares calculates the parameters that minimize the cost function:

$$\hat{\theta}_N = \arg \min_{\theta} \left(\frac{1}{N} \sum_{t=1}^N (y(t) - \varphi^T(t) \theta)^2 \right) \quad (3.15)$$

3.6 Model Validation

The calculated model that has fit the observed data best according to the chosen criterion must then be validated. Validation are tests to assess how well the model describes the variable to its purpose which includes reconstructing the output well enough from inputs with a different experiment than the one used to estimate the model. This way, deficient models are rejected and models that perform well gain a certain confidence, but it is worth noticing that no model represents the system perfectly.

3.7 Physical Modelling

When modelling a thermal system the two physical quantities of importance are heat transfer and temperature difference. In fact heat transfer is essentially driven by temperature difference across a heat pathway which is a channel through which heat flows. Across these channels heat flow encounters discontinuities in material properties and depending on the physics of these discontinuities heat transfers in different modes: conduction, convection and radiation. Both conduction and convection follows the same mechanism, i.e., the same mathematical equation 3.17 describes both modes. Below are the definitions of each mode:

- conduction is heat transfer by diffusion.
- convection is heat transfer by a moving fluid (gas or liquid).
- radiation is heat transfer between two solids that are exposed to each other and exchange electromagnetic energy as governed by Stefan Boltzmann Law.

Similar to electrical circuits thermal systems can also be represented by thermal circuits, i.e., the system can be modeled as thermal elements that interact by the laws of thermodynamics. Below is a table of electrical elements and their thermal counterparts:

Electrical component	Electrical SI unit	Thermal component	Thermal SI unit
Resistance	Ω	Thermal resistance	K/W
Capacitance	F	Heat capacity	J/K
Voltage difference	V	Temperature difference	K
Current	A	Thermal power	W

Table 3.1 Electrical components and their thermal counterpart [5].

A heat capacity stores thermal energy at a temperature difference when the stored energy at a reference temperature is set to zero. An example of a heat capacity is a block of aluminum between two different temperatures. In the same way as electrical resistors provide a pathway for electrical charges, thermal resistors provide a pathway for heat flow also driven by temperature difference ,e.g, a boundary between a solid and a fluid. A temperature source is a fixed temperature at a point regardless of the heat flow rate, similar to batteries. An example of a temperature source is a temperature regulator. Expectedly, thermal resistors in series or parallel are summed in the same manner as electrical resistors.

3.7.1 Lumped capacity systems

The notion of heat capacity and thermal resistor assumes a degree of approximation ,e.g, when treating a block of a metal at a temperature difference as a heat capacity the temperature would in reality vary across the block itself. However, assuming that heat transfer across the block is much faster than across the boundary, the concept of lumped capacity system can be introduced. This concept means that finite thermal objects are considered at some average temperature although in practice temperature variation exists across the object. Another concept that is closely related to lumped capacity and in fact is a metric that decides the applicability of lumped capacity is the Biot number. It gives information about the uniformity of heat transfer in a lump, i.e, a low Biot number means that the thermal lump heats or cools uniformly and consequently the object can be treated as a lumped capacity. The Biot number is thus the ratio of the conductive to convective resistance.

$$Bi = \frac{h}{k}L \quad (3.16)$$

- k: thermal conductivity [W/(m K)]
- h: convective heat transfer coefficient [W/(m²K)]
- L: characteristic length [m]

When treating a thermal system according to the lumped capacity model the number of nodes (lumped capacity objects) decides the degree of complexity one wants to capture, i.e pouring hot water in a mug initially at room temperature and regarding the mug-hot water system as one node will only capture the temperature data leading to equilibrium of the whole system and will not give information about temperature record of the mug and hot water separately. In contrast, if the mug and hot water were to be regarded as two nodes one could record both the rising temperature of the mug and the cooling of the water.

Simscape is a tool in Matlab that enables creating physical models from physical components that interact with each other in a Simulink environment. Simscape has a thermal library that includes all the thermal components in table 3.1 and they all obey pre-programmed thermal laws:

$$Q = \frac{\Delta T}{R} \tag{3.17}$$

and

$$Q = m \cdot c \cdot \frac{\Delta T}{T_s} \tag{3.18}$$

R is either convective or conductive thermal resistance depending on the the heat transfer across the thermal boundary. A schematic example illustrating all the thermal components discussed as well as other ones can be seen in fig. 3.2. This is a one node model, i.e there is only one thermal capacitance.

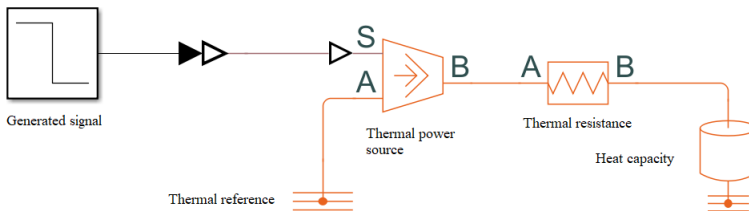


Figure 3.2 Simscape schematic of a heat power source applying thermal power by conduction/convection to a thermal capacitance through a thermal resistance.

3.8 The Inverse

Three methods are adopted to acquire an inverse model of the calorimeter. Firstly, a direct model S_D is identified from the input/output data. This means that the electrical signal generated in the sand ampoule is treated as input and the thermal power measured is treated as output. The electrical signal is not sampled by the instrument but rather constructed manually and noise-free in Matlab. Thus the input and the output are not affected by the same noise source and noise is only detected on the output. The set of models identified are mathematically inverted, given that an inverse exists, to produce the inverse model S_D^{-1} . The second method attempts to estimate an inverse S_I directly from the data. The measured power is now treated as input and the electrical signal is treated as output. The last inverting method makes use of the physical model and the inverse is calculated from the algebraic and difference equations from the output to the input. The three methods are summarized in fig 3.3

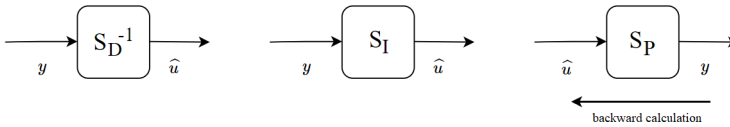


Figure 3.3 Inverse systems of the three methods.

3.8.1 Difficulties with the inverse

A problem that arises when inverting an LTI system is when the inverse system is unstable or uncausal. In control theory the system is characterized to be minimum phase if both the system and its inverse are causal and stable. A system is minimum phase if and only if the poles and zeros of the z -transform of the system are inside the unit circle. It is thus apparent that the flexibility of choosing the zero placement in the direct system S_D is restricted to inside the unit circle. Such a condition makes it difficult to estimate a forward model that meets high accuracy criterion to later be inverted to model that might not be physically correct.

4

Implementation of the Forward Inverse Model and the Estimated Inverse Model

4.1 Collecting data

4.1.1 Design limitations

For the purpose of collecting measurement data for the identification procedure, the ability to design the experiment, i.e., design and apply the desired input, is essential for a successful identification. The instrument at hand is equipped with a fixed heater in the ampoule holder for calibration purposes, but it is disadvantaged with the limitation that it is programmed to only send pulses at a fixed rate (which was not available at the time of study) or signals that resemble a long term cement measurement output. Another disadvantage is the location of the fixed heater which is not in the sample. In a hydration reaction, heat is produced from within the sample which is not the case with a fixed heater. A mobile heater however can be placed in the reaction zone (in the sample) which is more accurate than a fixed heater [8]. The mobile heater used is built of four $100 \pm 1 \Omega$ resistors coupled in an arrangement depicted in fig. 4.1 This arrangement was implemented to try to dissipate heat evenly in the sample so as to create the geometry of the cement reaction. Furthermore, the instrument only allows sampling at a 5 s rate which may lead to down-sampling of the fast dynamics of hydration when a cement ampoule is inserted. Consequently, when exciting the system with an input pulse, one cannot be certain that there is not a time delay between the input and output. It is assumed in this report that a delay does not exist.

The input signal (thermal power, P_{in}) is restricted to pulses with amplitudes deter-

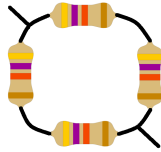


Figure 4.1 Mobile heater made of resistors. Attention should only be paid to the arrangement and not the resistor values (they do not depict the actual values).

mined by the a resistor circuit outside the calorimeter and a 20 V voltage U . Figure 4.2 represents the circuit:

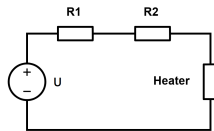


Figure 4.2 Outer pulse generating circuit

The voltage applied to the heater is calculated according to equation 4.1:

$$P_{in} = \frac{\left(U \frac{R_{Heater}}{R_1 + R_2 + R_{Heater}} \right)^2}{R_{Heater}} \quad (4.1)$$

4.1.2 Designing the experiment

As mentioned above the input signal is not sampled in the calorimeter. Instead the input pulses are created noise-free digitally in Matlab. Three types of input signals were generated. The first one is a step signal in both directions that allows the output measurement to reach steady state, the second are short duration pulses with different rates that do not allow the output measurement to reach steady state, and the last signal is in fact not electrical, but is a single pulse that is created by charging an ampoule with a sand sample that has a temperature higher than the calorimeter. Examples of these signals and their output measurements are shown in fig. 4.3 below.

These graphs do not show the noise when change rate is low in measurement signals. If one is to zoom in on the first step-signal in the output in (b) in fig. 4.3 one can clearly see the signal is embedded in very low noise. Figure 4.4 illustrates this.

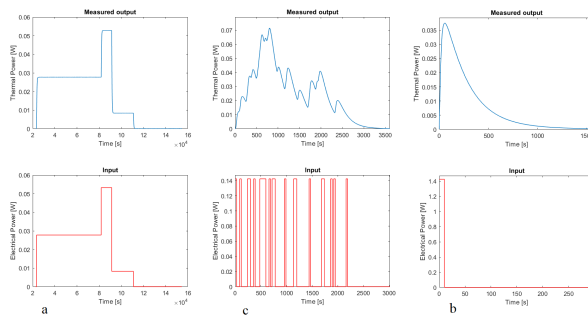


Figure 4.3 From the left: a steady state stair signal, pulses with different rates and a sand ampoule signal.

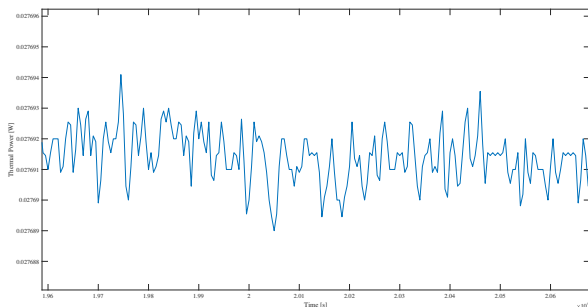


Figure 4.4 Noise seen on steady states level.

4.1.3 Selecting first model structure

As discussed in section 3.3.1 there are several standard model structures that tend to be enough to describe most linear systems. Many of them are found in SITB and can be used with different orders and different input/output delays. There are even models that can include non-linearity descriptions such as *Non Linear ARX models*. With so many structures and degrees of freedom, in terms of model order and delay samples, to choose from it is difficult to decide what model structure to start at. Luckily there are several books, for example [2] that provide some guidelines for the repetitive identification approach. A common first approach is to start with estimating several combinations of ARX models. This is a feature available for both ARX and *state space* structures. The SITB then returns a histogram of the the models' ratio of prediction error variance to the output variance. The lower the ratio the more accurate the model is in explaining the dynamics. The fit percentage is computed with regard to a validation data that differs from the estimation data. Usually models with unexplained prediction variance values close to the best model are also

worth to examine. Once models are picked they are further examined by looking at their frequency response, transient response, noise spectrum and model residuals. These function can give insight into the model dynamics such as the order of the system, the time delay that are exploited to further develop the model or try new structures. Two important functions to examine in order to acquire good models are the model fit percentage and the model residuals.

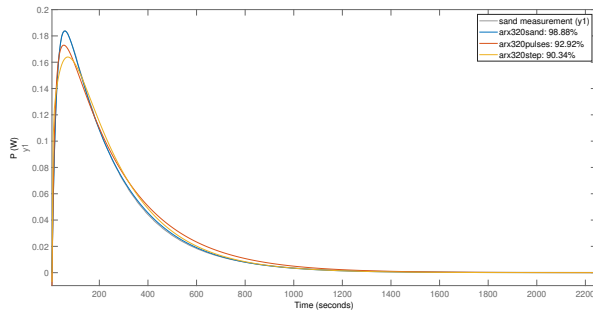
Output fit. Computes the root of the mean square value of the difference between measured and simulated output. High percentages indicates high model fit for the validation data but does not necessarily mean that the model is good enough and would score the same value on different data. Therefore it is also as important to analyze the residuals.

The residuals. An arbitrary linear model can be written as

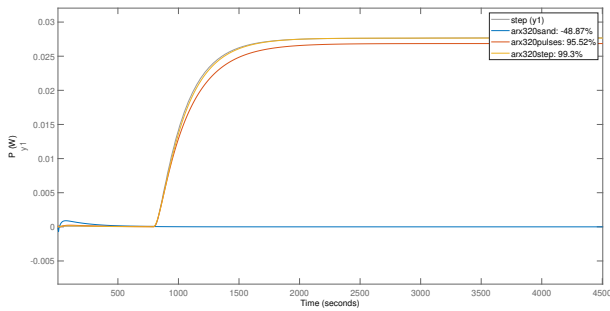
$$y(t) = G(q)u(t) + H(q)e(t) \quad (4.2)$$

In a perfect model, the noise $e(t)$ represents the part, residuals, that the model could not reproduce from the input. Thus, a good model should not display dependency between the input and residuals (cross correlation), also the residuals should be mutually independent (auto correlation). Both tests should consequently be done to ensure that these correlation functions are within or at least not significantly outside the confidence interval. A rule of thumb when trying to optimize the model to meet the correlation conditions is if the cross correlation varies slowly outside the confidence interval which indicates few poles in the model, while sharp peaks means few zeros or delays.

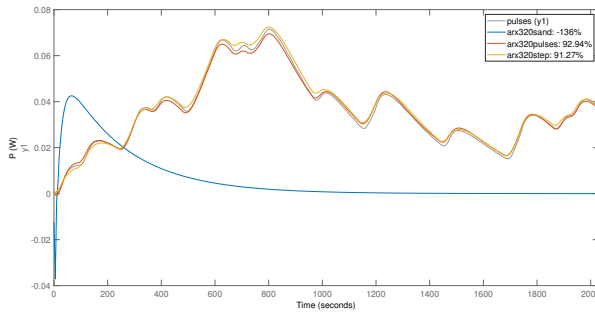
ARX. As suggested earlier different experiments will be tested to estimate the model, it is therefore natural to validate each estimated model on the remaining data sets fig. 4.3. In this example we do not consider inevitability of the model but only try to answer the question which data set is most suitable for direct-model estimation. An ARX with three poles and two zeros was used as it was the lowest order that captured the low order dynamics. Model arx320step is estimated on 4.3 (a), model arx320pulses is estimated on 4.3 (b) and model arx320sand is estimated on 4.3 (c). Figure 4.5 shows the responses of ARX320 to the input signals in 4.3. Clearly the sand pulse data is not informative enough to capture higher order dynamics. The ARX model estimated on this data fails to simulate the measurements of both the stair signal and the short pulses. It is therefore disregarded for estimation and can only be used for validation. The other two data sets seem to perform almost equally well and will be used henceforth for estimation and validation.



(a) ARX320 model response to a sand pulse.



(b) ARX320 model response to a step.



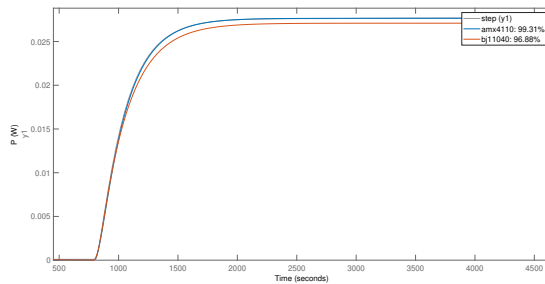
(c) ARX320 model response to short pulses.

Figure 4.5 Model fits of the same model (ARX320) but estimated on different data sets.

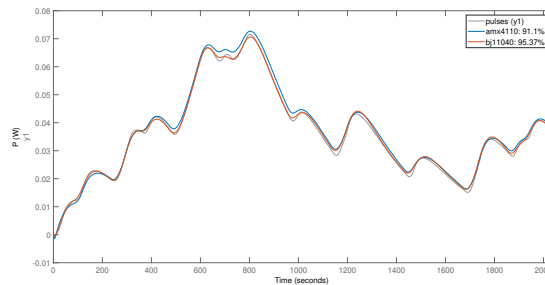
4.1.4 Developing the Model

The first step gave an intuitive idea of the model order and which estimation is the most informative. The next step is to include a more flexible noise model utilizing

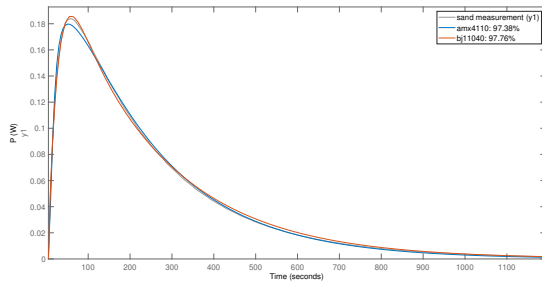
a BJ or ARMAX structure and analyse both the auto correlation and cross correlation functions. At first, the main approach was to acquire a good direct model that satisfies a high fit percentage and passes the whiteness and independence test within the confidence intervals. However, some models, as good as they are, might not have an inverse or they have an unstable inverse. Therefore, the forward models in fig. 4.6 are estimated on the cost of first satisfying invertibility and then stability. The BJ11040 model was estimated on the first half of the short pulses in fig. 4.3 and AMX4110 was estimated on the four step signal in the same figure. When analysing the residuals it is important not to validate on data sets with too many samples and little input excitation, i.e., the sand pulse measurement is originally 1000 samples and is only excited on a pulse of one sample length. Validating on the whole data set will give bad confidence unless the data set is reduced. As mentioned above, to enable invertibility the correlation functions are allowed to cross the confidence interval as seen in fig. 4.7



(a) Direct models response to a step signal.

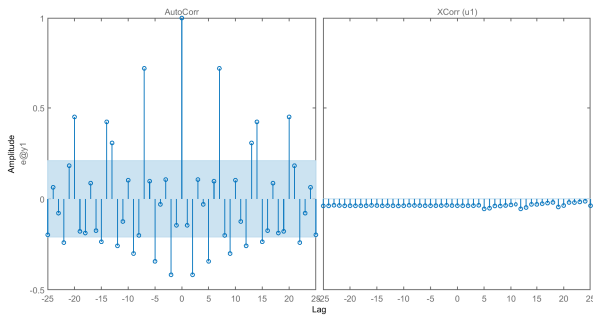


(b) Direct models response to pulses.

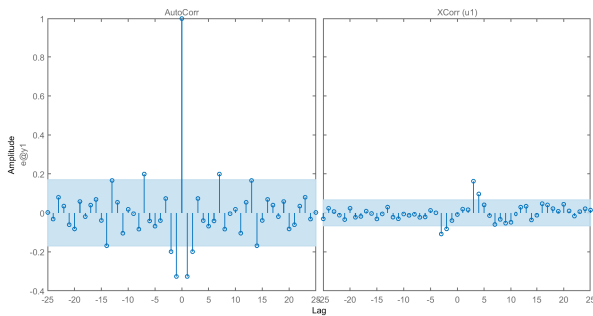


(c) Direct models response to sand pulse.

Figure 4.6 Direct model response to different validation sets.



(a) AMX4110 auto correlation and cross correlation analysis.



(b) ARX412 auto correlation and cross correlation analysis.

Figure 4.7 Residual analysis of the direct models.

4.1.5 Inverting the Forward Models

The two direct models are then inverted mathematically. To evaluate the inverse models one can validate them against some validation data sets. However, one can not conclude from, i.e., the normalized root means squared error (NRMSE) value if these models are good enough. One can instead use measurement data as input to the inverse models and examine if the original input is reconstructed. In the case of the measurement of the cement sample the input is sought and the only way to validate the models is to feed the measurement signal to a cascade coupling of the forward and inverse model and examine the output fits the measurement signal. The method is shown in fig. 4.8 . For visualisation purposes the response of the two inverse models to the measurement data was filtered in fig. 4.9. The filter used is a Savitzky-Golay filter of order one and a 7 samples window.

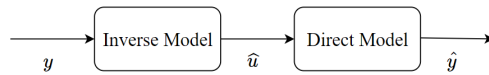
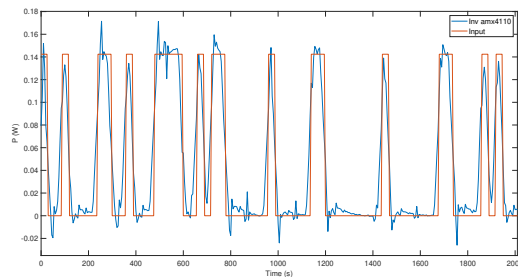
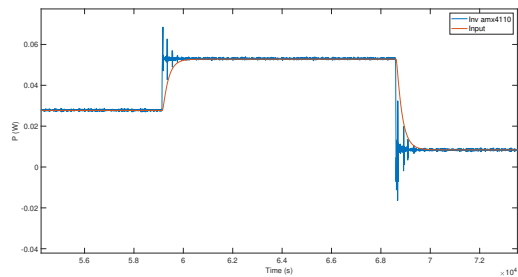


Figure 4.8 Cascade coupling of the direct and inverse models.



(a) Response of BJ11040 model inverse.



(b) Response of AMX4110 model inverse.

Figure 4.9 Inverse models response.

Chapter 4. Implementation of the Forward Inverse Model and the Estimated Inverse Model

The reconstructed input signal from the inverse model response to the cement measurement can be seen in fig. 4.10 and 4.11. It is clear that these signals can not represent the original hydration reaction although feeding each response to its respective forward model does recreate the measurement to about 99%. However if signals were fed to another forward model they do not reconstruct the measurement as seen in 4.12. If the first 100 seconds are disregarded on can observe an exponential decrease in the signal which can represent the heat rate from the hydration reaction.

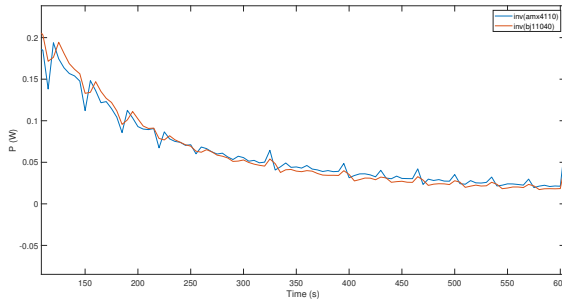


Figure 4.10 Input signal reconstructed from inverse models inverted from forward models.

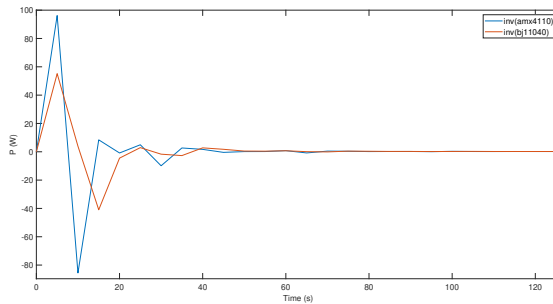


Figure 4.11 First 100 unfiltered seconds of the estimated inverse models response to a cement measurement.

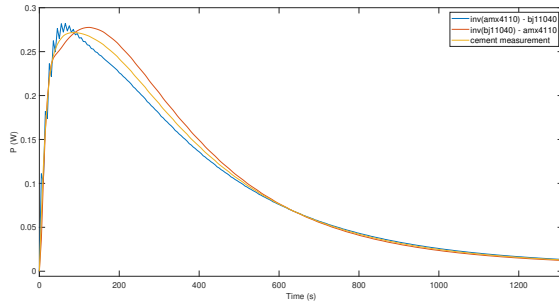


Figure 4.12 Reconstructed output from the cascade coupling of inverse models then forward models.

4.1.6 Direct estimation of the Inverse Model

In this section, the inverse is estimated using the same approach as estimating the forward model. The measurement will be regarded as inputs and the inputs will be regarded as outputs. In addition to classical linear models discussed in chapter 3 the IARX model structure will also be tested. Figure 4.13 and 4.14 shows the reconstructed input from estimated inverse models.

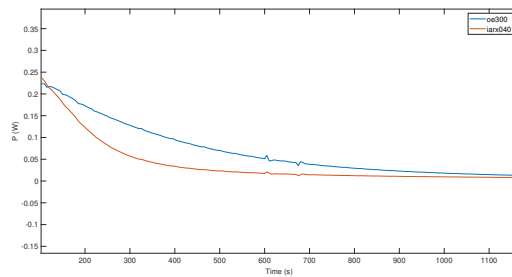


Figure 4.13 Input signal reconstructed from directly estimated inverse models (filtered).

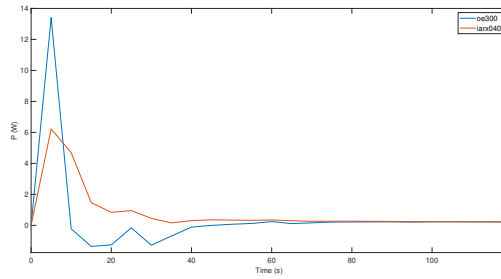


Figure 4.14 Input signal reconstructed from directly estimated inverse models (first 100 unfiltered seconds).

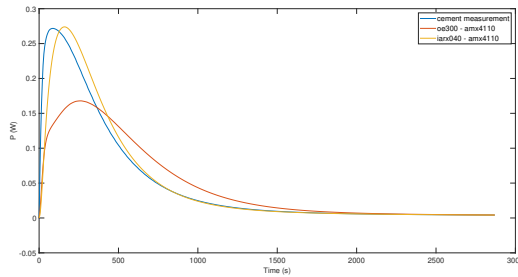


Figure 4.15 Response of AMX4110 to input reconstructed from OE300 and IARX040.

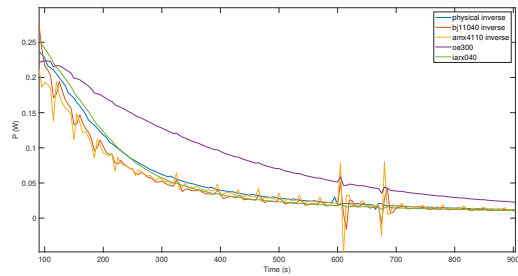


Figure 4.16 Response from all the inverse models (filtered).

Model OE300 was estimated on the short pulses data, see 4.3 and when using this model in a cascade coupling with the forward model AMX4110, which is estimated on the step data, it did not reconstruct the cement measurement well. One can also see in fig. 4.16 that OE300 is the only model that had a slower decrease.

All the other inverse models had approximately the same decrease rate.

To conclude, estimating the inverse directly from the data or from the forward model did not succeed in explaining the temperature difference that the cement sample had prior charging in the instrument. However, most of the inverse models showed a similar decrease heat rate after 100 s and this could represent the true heat rate from the hydration reaction. The choice of the estimation data was also important when the inverse model was estimated directly from the data. When the short pulses data was used to estimate an inverse, the response from the model did not agree with the rest of the estimated inverse models.

5

Physical Modelling Implementation

Knowledge of the physics and geometry of the I-Cal Ultra calorimeters allows to use physical modelling. The geometry of the profiles of our instrument, and even the electrical specification of the components used, are well known. However, perfect modelling is still not feasible. The difficulty arises because of the numerous heat pathways and heat transfer modes in the system. It is indeed possible to make an FEM-model of the system with tools such as COMSOL but these complex models are not suited to be integrated in evaluation software for PolabCal. The better alternative is to use LHCM as explained in 3.7.1.

5.1 Nodal Models

The model structure in LHCM is defined by the number of nodes N . Our approach is to select the nodes in a fashion that the first nodes start at the input and successively model the system heat capacities as nodes along a pathway that ends at the output (calorimeter measurement). This way we are mostly accounting for heat transfer from the input to the output and ignoring heat losses in the rest of the pathways. Three models with three, four and five nodes respectively will be simulated and they are depicted in fig. 5.1. As expected the number of parameters is $2 \cdot N$ as between each two nodes there has to be a thermal channel represented by a thermal resistance. Table 5.1 explains the parameter labels in fig. 5.1.

Label	Physical part	Label	Physical
S	The sample	A	Thermal resistance between S and A
A	Ampoule	AX	Thermal resistance between A and X
X	Ampoule holder	XH	Thermal resistance between the X and H
H	Heat sink	HR	Thermal resistance between H and R
R	The reference	H0	Thermal resistance between H and the ref. temperature

Table 5.1 Parameter labels and their representation in I-Cal Flex.

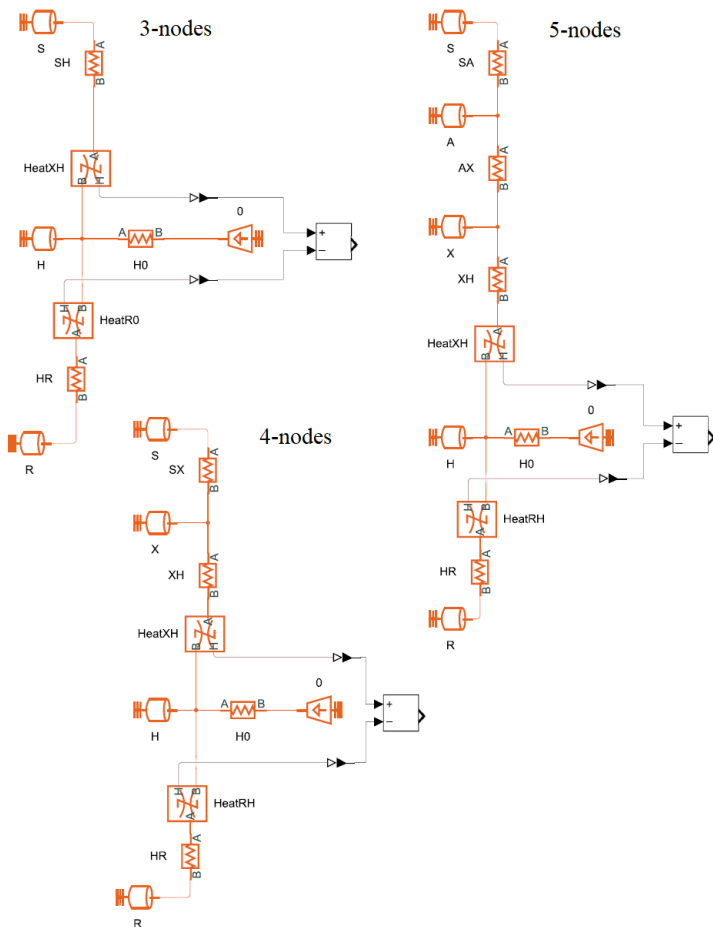


Figure 5.1 Simscape lumped heat capacity models of 3, 4 and 5 nodes.

5.2 4-nodes Model

The initial guess of the model parameter values was calculated based on knowledge of material property and the dimensions of the geometric parts (not given here). Of course one needs an experiment to validate the model and for this purpose a drop of an ampoule with sand mixed with water and with initial temperature different from the temperature of the calorimeter will be our main experiment in physical modelling. Simscape offers a variety of useful boxes and features for this kind of experiment, e.g., in the 4-nodes model one can set the initial temperature of the sample node to that of the experiment and examine how well the simulated output

signal matches the measurement. Figure 5.2 shows the simulated output from the initial parameter values and the measured signal of a sand mixed with water sample of 2.72 K over-temperature. The simulated output from the 4-nodes model does not match the measurement at all and this is quite expected when the model was solely based on hand calculation and approximation of heat pathways and capacities. At this point applying a grey box optimization technique will result in heavy processor calculation that may or may not converge to a minimum. Rather, analysing the sensitivity of the parameters could save some computing power and give insight into which parameters influence the output of the model most.

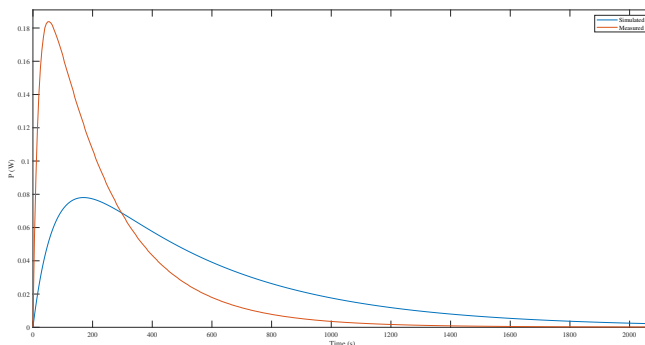


Figure 5.2 Simulated output (4-nodes) and measurement of a sand mixed with water sample with over temperature of 2.72 K.

5.2.1 Sensitivity Analysis

The initial parameter values could be used as means to normal distribution with user defined variance to generate parameter sets for the sensitivity analysis. However, we choose a uniform distribution instead to examine if the initial parameter guess is robust enough. The number of parameter sets is set to $10 \cdot N$ resulting in 80 parameter sets. For each parameter set the value of the cost function, signal matching, is calculated and correlation is computed. Figures 5.3 and 5.4 illustrate the results. Both graphs show that parameters S, X, SX and XH are of greatest influence. Note that a higher SignalMatching value means higher violation of the requirement.

Parameter optimization can now be conducted only on these parameters and the simulated response of the same experiments after optimization is shown in fig. 5.5.

Visually, one can see good signal matching and therefore optimizing now on all parameters could most probably converge to a minimum. Figure 5.6 displays the final optimization results. The parameter values at each step are listed in table 5.2.

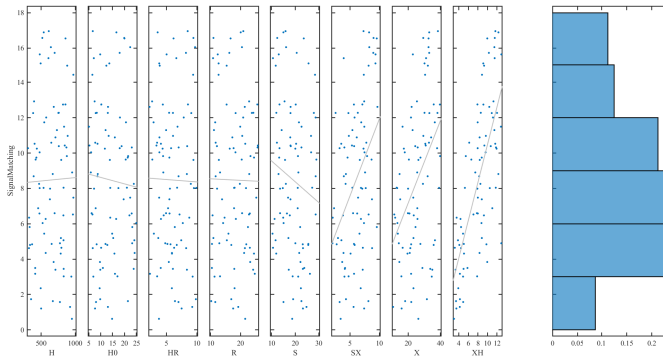


Figure 5.3 A scatter plot of all parameter sets and the requirement value. The line fitted represents the correlation. The histogram graph displays the probability distribution of the signal matching values

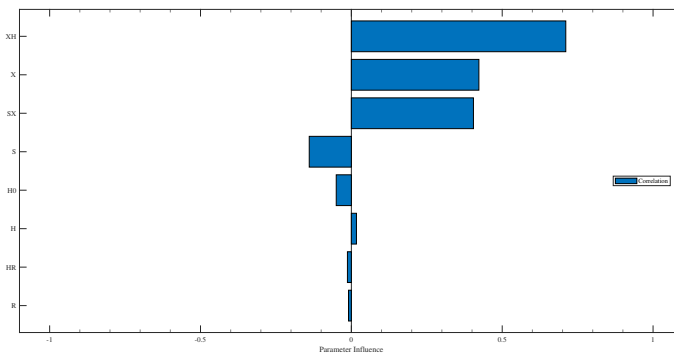


Figure 5.4 A tornado graph of parameter influence on signal matching.

	Initial guess	After sensitivity analysis	Final optimization
S	21	19.65	19.78
X	30	8.02	8.22
SX	7	6.41	6.34
XH	9	4.5	4.5
H	700	Unchanged	465.5
R	21	Unchanged	16.54
HO	17	Unchanged	10.1
HR	7	Unchanged	7.8

Table 5.2 Parameter estimation.

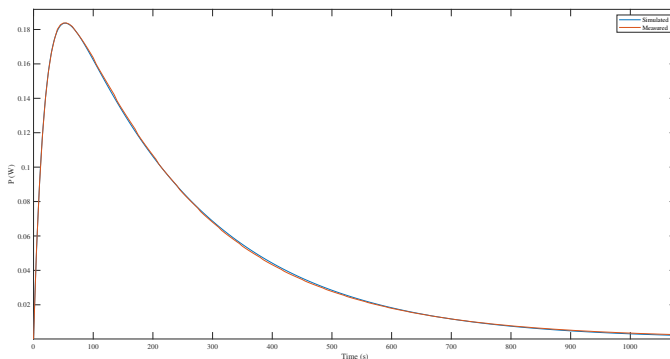


Figure 5.5 Measurement and simulation (4-nodes model) after optimizing on S, X, SX and XH.

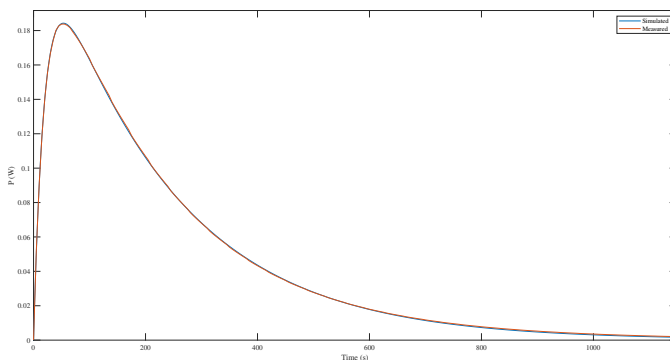


Figure 5.6 Measurement and simulation (4-nodes model) after optimizing on the most sensitive parameters and then on all parameters.

5.3 5-nodes Model

Similarly, we apply the same steps as for the 4-nodes model: initial guess, sensitivity analysis, optimization on the most sensitive parameters and a final optimization on all parameters. The results for the middle steps are similar and will not be presented only the final optimization is shown in fig. 5.7.

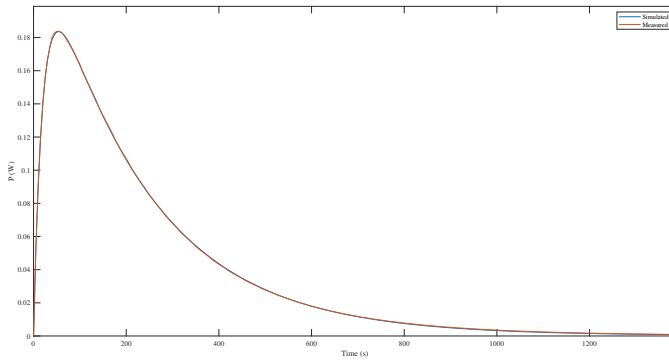


Figure 5.7 Measurement and simulation (5-nodes model) after optimizing on all parameters.

5.4 3-nodes Model

The 3-nodes model is essentially 3 heat capacities of which, based on our experiment, heat from over temperature in the sample flows through a resistance directly into the heat sink hence the absence of the initial rise in thermal power seen in the simulation output in fig. 5.8. As a result a minimum of two nodes before the heat sink is needed to capture the simplest dynamics of the system.

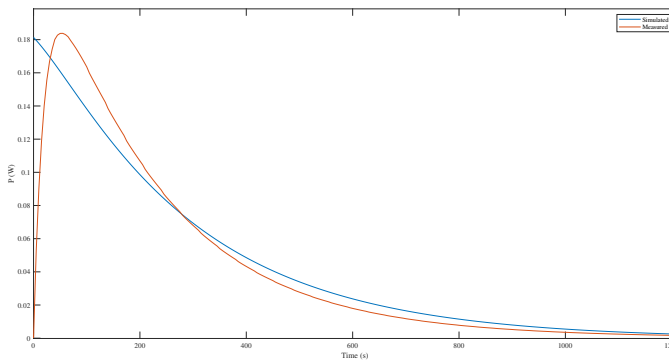


Figure 5.8 Measurement and simulation (3-nodes model) after optimizing on all parameters.

5.5 Comparison

Figures 5.6 and 5.7 looks much alike and it is difficult to distinguish visually which model is more accurate, but they both show a significantly better fit than fig. 5.8. The RSS of each model output and measurement in table 5.3.

	RSS
3-nodes	0.0748
4-nodes	$4.8 \cdot 10^{-5}$
5-nodes	$2.38 \cdot 10^{-5}$

Table 5.3 RSS of all three physical models.

5.6 Calculating the Inverse

The RSS of the 4-nodes model is $4.8 \cdot 10^{-5}$ which is only slightly higher than the 5-nodes model and has 2 parameters less. It will thus be used to calculate the input. This method is essentially equivalent to inverting a model mathematically with the difference that one can observe the rest of the variables in the system such as temperature. For instance, in fig. 3.2 if the temperature rise in the heat capacity at the first step is known one can through equations 3.17 and 3.18 compute the heat rate that caused the temperature rise. Adopting this procedure, the heat rate developed in a cement sample can be calculated through the 4-nodes model. This is useful to also acquire the initial temperature of the cement sample when dropped in the instrument. To make calculation easier, the reference node R together with thermal resistance HR will be ignored without significant change in parameter values when re-estimated, see table 5.4. Figure 5.9 shows the calculated inverse response to both a sand and cement measurement. The same figure is divided into fig. 5.10 and 5.11, that show the first 100 seconds and the time span 40-600 s respectively. This is to emphasise the exponential behaviour of the cement signal that cannot be seen in figure 5.9. Furthermore, to remove the periodic spikes from the signals in 5.10 a Savitzky-Golay filter of window-size 35 s (7 samples) is applied, see fig. 5.12. It is important to use the filter only on the second part of the signal (40-600 seconds) with the periodic behaviour because otherwise the first samples of the signal would be underestimated. One can see the distinction between the recalculated inputs of sand and cement measurements in figures 5.9-5.12. The sand input resembles a pulse while the cement input starts as a pulse but then decays quiet sharply.

Optimized parameters w/o reference	
H	579.99
H0	12.968
S	20.395
SX	6.668
X	9.5364
XH	4.1915

Table 5.4 Parameter values of 4-nodes model w/o reference.

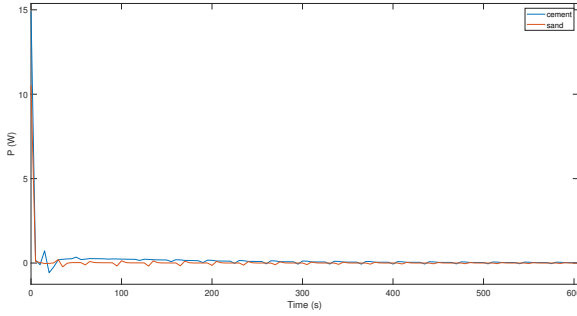


Figure 5.9 Calculated inverse response to a sand measurement and a cement measurement (unfiltered).

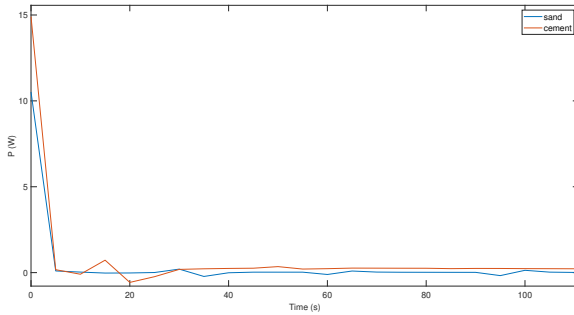


Figure 5.10 Calculated inverse response to a sand measurement and a cement measurement (first 100 unfiltered seconds).

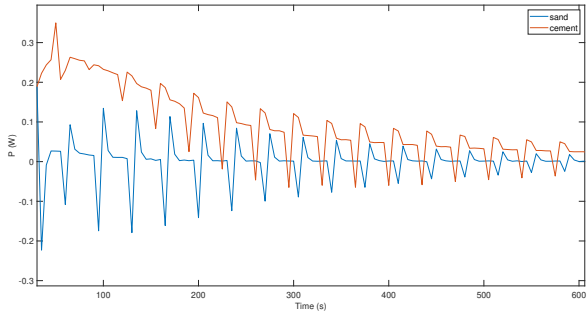


Figure 5.11 Calculated inverse response to a sand measurement and a cement measurement (unfiltered).

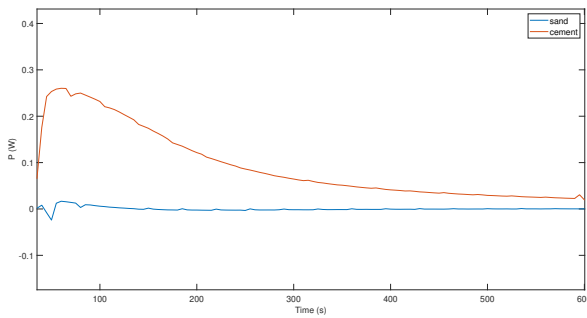


Figure 5.12 Calculated inverse response to a sand measurement and a cement measurement (filtered).

6

Discussion

The goal of the project was to find the original heat rate of the hydration reaction of cement with water. The interest was in extracting more information from the reconstructed input signal through inverse modelling. This means that neither the forward model nor the inverse model was intended to be implemented in some control policy and therefore the output from the inverse model should reflect some physical information. The two principal methods adopted were to build an inverse model through first, implementing a forward model with system identification and physical modelling and then to invert them, and the second method was to estimate the inverse directly by system identification. Although much work was done to collect informative data to estimate a good forward model, the results showed that the inverse of the forward model did not reconstruct the input in a physical manner. However, the forward models were useful, albeit only in validation in the cascade coupling. Estimating the inverse model directly was more successful and the results showed a more realistic heat rate curve that starts with high value and then decays. The IARX new feature of using future exogenous output was not exploited as the best model estimated did only use past outputs. It is also worth to notice that the inverse models estimated did not use any past inputs and can thus be regarded as impulse response models. The inverse models estimated with system identification gave indications of the true heat rate, at least after 100 s as most of them agreed approximately on the decrease of the true heat rate. The importance of the physical model was demonstrated in tracking where the source of the periodic spikes of the reconstructed input, see fig. ??, regardless from the method used. When the physical model was fed with a cement measurement one could track the calculation of the input from the output and follow all other quantities at each node and thermal pathway.

Appendix

Forward Model Parameter Values

arx320sand

$$A(q) = 1 - 1.412q^{-1} + 0.1564q^{-2} + 0.262q^{-3}$$

$$B(q) = 0$$

arx320step

$$A(q) = 1 - 2.011q^{-1} + 1.129q^{-2} - 0.1155q^{-3}$$

$$B(q) = 2.081 \cdot 10^{-5} + 0.001822q^{-1}$$

arx320pulses

$$A(q) = 1 - 2.4q^{-1} + 1.876q^{-2} - 0.4751q^{-3}$$

$$B(q) = -5.108 \cdot 10^{-6} + 0.001225q^{-1}$$

bj11040

$$B(q) = 0.001154$$

$$C(q) = 1 + 0.9316q^{-1}$$

$$F(q) = 1 - 1.8q^{-1} + 0.08628q^{-2} + 1.297q^{-3} - 0.5824q^{-4}$$

amx4110

$$A(q) = 1 - 2.76q^{-1} + 2.714q^{-2} - 1.108q^{-3} + 0.1549q^{-4}$$

$$B(q) = 0.0006621$$

$$C(q) = 1 - 0.08796q^{-1}$$

oe300

$$B(q) = 210.6 - 397.4q^{-1} + 187.8q^{-2}$$

iarx040

$$B(q) = 99.93 - 113.74q^{-1} + 18.31q^{-2} + 33.05q^{-3}$$

Bibliography

- [1] L. Ljung. *System identification : theory for the user*. Prentice-Hall information and system sciences series. Prentice Hall, 1999. ISBN: 0136566952.
- [2] L. Ljung. *System identification toolbox: for use with matlab: user's guide: version 5, mathworks*. https://instruct.uwo.ca/engine-sc/391b/downloads/IDENT_T.B.PDF. Accessed: 3 September 2022.
- [3] A. M. Neville. *Properties of concrete*. Longman Group, 1995. ISBN: 0582230705. URL: <https://ludwig.lub.lu.se/login?url=https://search.ebscohost.com/login.aspx?direct=true&AuthType=ip,uid&db=cat07147a&AN=lub.1153310&site=eds-live&scope=site>.
- [4] A. Oliveira, C. Zacharie, B. Remy, V. Schick, D. Marechal, J. Teixeira, S. Denis, and G. Michel. “Inverse arx (iarx) method for boundary specification in heat conduction problems”. *International Journal of Heat and Mass Transfer* **180** (2021), p. 121783. DOI: 10.1016/j.ijheatmasstransfer.2021.121783.
- [5] G. Sidebotham. *Heat Transfer Modeling: an Inductive Approach*. Springer International Publishing AG, 2015. ISBN: 9783319145136.
- [6] T. Solidia. “Chatham house patent-landscape report examines innovations in low-carbon cement and concrete, including solidia technologies’.” *Business Wire (English)* (2018). URL: <https://ludwig.lub.lu.se/login?url=https://search.ebscohost.com/login.aspx?direct=true&AuthType=ip,uid&db=bwh&AN=bizwire.c85333285&site=eds-live&scope=site>.
- [7] A. K. Tangirala. *Principles of System Identification : Theory and Practice (version First edition)*. Boca Raton FL: CRC Press an imprint of Taylor and Francis., 2014. ISBN: 1439895996.
- [8] L. Wadsö. “Operational issues in isothermal calorimetry”. *Cement and Concrete Research* **40**:7 (2010), pp. 1129–1137. DOI: 10.1016/j.cemconres.2010.03.017.

Bibliography

- [9] H. Zhang. *Building Materials in Civil Engineering*. Woodhead Publishing, 2011, pp. 7–423. ISBN: 9781845699550.

Lund University Department of Automatic Control Box 118 SE-221 00 Lund Sweden		<i>Document name</i> MASTER'S THESIS	
		<i>Date of issue</i> October 2022	
		<i>Document Number</i> TFRT-6186	
<i>Author(s)</i> Hassan Alzeidi		<i>Supervisor</i> Lars Wadsö, Dept. of Building & Environmental Technology, Lund University, Sweden Anders Rantzer, Dept. of Automatic Control, Lund University, Sweden Bo Bernhardsson, Dept. of Automatic Control, Lund University, Sweden (examiner)	
<i>Title and subtitle</i> Modelling of a Heat Conduction Calorimeter Used in Cement Plant Automation			
<i>Abstract</i> A model is used to describe a system physically or mathematically and to give information about changes in the system variables. Physical knowledge about the system and its quantities can be useful to build a physical model obeying the laws of nature. However, if the system is to be regarded as a black box with only input and output signals, system identification can be used to fit a mathematical model to describe the relation between the signals. The signals are usually physical quantities but the estimated model parameters do not necessarily reflect physical aspects of the system. The goal of estimating a model is either to calculate the effect given the cause, such models are called forward or direct models, or to calculate the cause given the effect, which is the objective of this thesis. These models are called inverse models and are widely used in heat conduction problems, e.g., estimating the heat flow rate at the source given measured temperature at a point. In this thesis the goal is to estimate the true heat flow rate from the hydration reaction in a cement sample when mixed with water from heat rate measurements in the isothermal calorimeter I-Cal Flex. The problem with such measurement is that it starts only after about 20-30 seconds, which is the time it takes for mixing the water and cement in an ampoule and charging it in the calorimeter. Under that time the cement sample temperature rises due to heat produced from the chemical reaction. The measurement process is automated in a robot called PolabCal and the measurement signal could possibly be used to control cement plants. The problem is that the measurement both includes the heat rate from the over-temperature that sample gained prior charging in the calorimeter and information about the dynamics of the instrument. There is therefore an interest in the pure heat rate from the cement hydration reaction as it is believed to be more informative than the measurement signal. Estimating the inverse model in this thesis was made by evaluating three methods; to estimate a forward model then to invert it, to estimate an inverse model directly from inputs and output measurements, and lastly to build a physical forward model and then use it to calculate the input.			
<i>Keywords</i>			
<i>Classification system and/or index terms (if any)</i>			
<i>Supplementary bibliographical information</i>			
<i>ISSN and key title</i> 0280-5316		<i>ISBN</i>	
<i>Language</i> English	<i>Number of pages</i> 1-52	<i>Recipient's notes</i>	
<i>Security classification</i>			

<http://www.control.lth.se/publications/>